COMPOSITE SCAFFOLDS ENRICHED WITH CALCIUM CARBONATE MICROPARTICLES LOADED WITH EPIGALLOCATECHIN GALLATE FOR BONE TISSUE REGENERATION

Krzysztof Pietryga[1,2*], Anca-Alexandra Panaite[3], Elżbieta Pamuła[1]

[1] AGH University of Science and Technology, Faculty of Materials Science and Ceramics, Department of Biomaterials and Composites, Al. Mickiewicza 30, 30-059 Kraków, Poland
[2] Silesian Park of Medical Technology Kardio-Med Silesia, ul. Marii Skłodowskiej-Curie 10C, 41-800 Zabrze, Poland
[3] University Politechnica of Bucharest, Faculty of Medical Engineering, Splaiul Independentei 313, 060042 Bucharest, Romania
*e-mail: pietryga@agh.edu.pl

Abstract

There is a need to develop advanced multifunctional scaffolds for the treatment of bone tissue lesions, which apart from providing support for infiltrating cells could assure the delivery of drugs or biologically active molecules enhancing bone formation. We developed composite scaffolds for bone tissue engineering based on gellan gum (GG) and gelatin (Gel) hydrogel enriched with epigallocatechin gallate (EGCG) loaded $CaCO_3$ microparticles and subjected to enzymatic mineralization with calcium phosphate (CaP). The method of manufacturing $CaCO_3$ microparticles was optimized. The EGCG-loaded microparticles were smaller than those unloaded, and the release of EGCG was prolonged for up to 14 days, as shown by the Folin-Ciocalteu test. The particles reduced the viability of the MG-63 cells as compared to the control. However, when they were loaded with EGCG, their cytotoxicity was reduced. The particles were suspended in a GG/Gel hydrogel containing alkaline phosphatase (ALP), soaked in calcium glycerophosphate (CaGP) solution to create CaP deposits, and submitted to freeze-drying, in order to produce a porous scaffold. The microstructure of the scaffolds was characterized by optical and scanning electron microscopy and showed that the size of the pores corresponds to that of the spongy bone. In vitro tests with MG-63 cells confirmed that mineralized scaffolds support cell adhesion and growth to a higher extent than nonmineralized ones.

Keywords: *gellan gum, gelatin, hydrogel, calcium carbonate microparticles, enzymatic mineralization, epigallocatechin gallate (EGCG)*

[Engineering of Biomaterials 166 (2022) 12-21]

doi:10.34821/eng.biomat.166.2022.12-21

Submitted: 2022-11-21, Accepted: 2023-02-10, Published: 2023-02-28

Introduction

Although bone tissue as such displays remarkable regenerative properties, bone tissue defects require special attention, especially for lesions with large size [1]. Today, tissue engineering approaches that apply scaffolds able to support adhesion, viability, and proliferation of cells to improve tissue healing are widely studied [2]. In this context, composite scaffolds, designed to mimic phase composition, structure, and properties of bone extracellular matrix, seem to be particularly promising [3]. Among the different approaches to producing such biomimetic scaffolds, one is especially interesting, which is based on the enzymatic mineralization of hydrogels [4,5]. Moreover, additional functionalities to stimulate bone tissue defects treatment, such as modifying scaffolds with drug delivery carriers, are of particular importance [6].

Gellan gum (GG) is an anionic calcium-binding polysaccharide produced by bacteria (*Sphingomonas elodea*) during aerobic fermentation; it is widely used in the food industry as a thickener and stabilizer [7]. More recently, GG submitted to mineralization has been applied as a bone tissue engineering scaffold [5,8]. In brief, mineralization of GG can be achieved by the addition of an enzyme, alkaline phosphatase (ALP), and incubation in a calcium glycerophosphate (CaGP) solution. The ALP uses the CaGP as the substrate, cleaving the phosphate, resulting in the precipitation of insoluble phosphate salts (CaP) inside the hydrogel.

Calcium carbonate microparticles due to their high surface-to-volume ratio, high specific surface area, easy synthesis, and ability to exist in a variety of morphologies and polymorphs are considered for medical applications, especially as drug delivery systems and as a mineral phase in polymer/ceramic composites [9,10]. They have been found to possess excellent biocompatibility with bone tissue and negligible cytotoxicity toward mammalian cells [9].

Epigallocatechin gallate (EGCG), belonging to a group of catechins, has been shown to have a pharmacological effect on bone metabolism, induce osteogenic differentiation, and inhibit osteoclastogenesis [11,12]. Despite the positive properties, its delivery to the bone tissue lesion is challenging.

The aim of this study was to develop innovative composite scaffolds for bone tissue engineering based on GG and Gel enriched with $CaCO_3$ microparticles loaded with EGCG and submitted to enzymatic mineralization and to test their microstructure, properties, and cytocompatibility with osteoblast-like MG-63 cells.

Materials and Methods

Materials and chemicals

All materials, including GG (G1910, "Low-Acyl", 200-300 kD), gelatin (G2500, from porcine skin), calcium glycerophosphate (CaGP, 50043), alkaline phosphatase (ALP, P7640), EGCG (E4143, >95%), and Folin-Ciocalteu reagents, were acquired from Sigma-Aldrich, unless otherwise stated. Calcium chlorate and sodium carbonate were purchased from Avantor Performance Materials Poland.

Particles preparation

Calcium carbonate particles were prepared by the precipitation method. The 0.33M Na_2CO_3 solution and the 0.33M $CaCl_2$ solution were mixed and immediately stirred with a magnetic stirrer or ultrasound. For the stirring method, two intensives were used: magnetic stirrer with 120 rpm (Ms120) and 1000 rpm (Ms1000) or sonicated (VCX 130 with 6 mm probe, Sonics & Materials, USA) at 20% and 60% amplitude (So20 and So60, respectively). The particles were centrifuged and washed 2 times with ddH_2O.

Hydrogel preparation

Hydrogels were prepared from GG and gelatin and cross-linked by $CaCl_2$ and containing ALP for the mineralization process. Smaller particles obtained by sonication were also added to the hydrogels. The procedure for obtaining hydrogels was as follows: GG, Gel, and $CaCl_2$ solutions were prepared and heated to 90°C for 30 min. The temperature was lowered to 70°C. The ALP solution in water and the suspension of particles in water were prepared. The gelatin solution was mixed with $CaCl_2$ and then with ALP solution (in H_2O), the suspension of particles, and finally GG. The solution was poured between two Petri dishes separated with 1 mm spacers. The final concentration of the ingredients in the hydrogel was: 0.5% w/v GG, 10% w/v gelatin, 0.03 % $CaCl_2$, 1 mg/ml ALP, and 0.15% particles with EGCG. The hydrogel was cooled to room temperature until gelation and then stored at 4°C for 30 min for further hardening. Cylindrical samples of 8 mm diameter and 1 mm height were cut.

Hydrogel mineralization

Right after the preparation, cylindrical 8 mm samples of the resulting hydrogel were incubated in 0.1M CaGP for one day. After mineralization, the samples were washed until the next day in ddH_2O to remove by-products.

Particle size distribution

The size of the microparticles was determined by light microscopy (Axiovert 40, Zeiss). Particles were prepared by dropping the suspension of diluted particles into a glass slide and collecting microscopic images in transmitted light. For each particle type, 500 particles were measured in ImageJ and the collected data was presented as histograms.

EGCG release test

The concentration of EGCG released from the particles was measured using the Folin-Ciocalteu method. The particles (10 mg) were incubated in 1 ml of PBS in a 24-well plate for 14 days. The supernatant was collected after 1 h and 1, 3, 7, and 14 days of incubation. For each measurement, 100 µl extract was mixed with 10 µl 20% Na_2CO_3 and 10 µl Folin-Ciocalteu reagent. The mixture was incubated for 30 min and then the absorbance was measured at 760 nm (FLUOstar Omega Microplate Reader, BMG LABTECH). The EGCG was calculated from the calibration curve in the range of 1-50 µM EGCG. For each interval, percentage release was calculated based on the initial measurement of the EGCG concentration in particles after complete dissolution in 0.1 M HCl.

Microstructure

The microstructure of the particles and freeze-dried hydrogels was analyzed by SEM microscopy (Hitachi S3400N, Japan). The material was mounted using carbon tape on holders. Observations were carried out under a low vacuum (70 Pa) without carbon sputtering. Before measurements, the hydrogels were frozen at -80°C and freeze-dried for 1 day. Additional microphotography of the freeze-dried hydrogel scaffold was recorded on AxioZoom (Zeiss, Germany) light microscopy. The images were taken in transmitted angular light.

Biological properties

Cytotoxicity and viability tests on osteoblast-like MG-63 cells (European Collection of Cell Cultures, Salisbury, UK) were performed in contact with particles. First cells were cultured in 100 µl Dulbecco's Modified Eagle Medium (DMEM PAA, Austria) supplemented with 2% fetal bovine serum (FBS), 1% penicillin/streptomycin, 2 mM L-glutamine, 1% non-essential amino acids in a 96-well plate (Nunclon). The particles (So20 and So60) were first incubated with 70% EtOH for 10 min for sterilization. Subsequently, the particles were washed 2 times with phosphate buffered saline (PBS) and resuspended in cell culture medium at concentrations of 10, 5 and 2.5 mg/ml. After the MG-63 cells confluence was reached, 10% of the suspension of particles was added to the cell culture. Cell culture with particles concentration of 1 mg/ml, 0.5 mg/ml, and 0.25 mg/ml was continued for 2 days.

Cytotoxicity was measured by the lactate dehydrogenase (LDH) test (Sigma-Aldrich) on medium collected from cell culture. 50 µl of medium was mixed with 50 µl reagent and the reaction was carried out for 15 min and then stopped by adding 50 µl of 0.1 M HCl. The absorbance was measured by the Tecan Sparck microplate reader at 492 nm.

Viability was tested by resazurin reduction (Alamar Blue, R7017, Sigma-Aldrich). Cell media from the cultures were removed and replaced by the same volume of media containing 0.05 mg/ml of resazurin. The culture was then continued for the next 4 h until a visible change of colour was observed. The fluorescence of the analyzed culture medium was measured for emission within 585 nm with extinction at 570 nm. Collected values were normalized to 100% viability of the control culture (cells without particles).

Viability, cytotoxicity, and morphology were additionally visualized by live-dead staining. The medium was removed from each well and replaced with a staining solution – 0.1% calcein AM (17783, Sigma Aldrich) and 0.1% propidium iodide (537060, Sigma-Aldrich) in PBS. After 20 min of incubation, fluorescence images were taken using AxioVert 40 with HXP 120 C metal halide illuminator (Zeiss, Germany).

Results and Discussion

Calcium carbonate microparticles

Calcium carbonate microparticles obtained by the precipitation method could be prepared relatively easily by mixing a Na_2CO_3 solution with a 0.33M $CaCl_2$ solution [9]. Particle precipitation is spontaneous, but particle size depends on the intensity of mixing (shear rate) (FIG. 1).

In our work, we tested two methods of mixing: magnetic stirrer and sonication. Magnetic stirrer at low speed (120 rpm) led to larger particles (median 7.5 µm) whereas fast stirring (1000 rpm) led to much smaller particles (median 3.5 µm) (FIG. 2). Similar particles as the latter (median 4 µm) could be obtained by ultrasound set to 20% amplitude. Much smaller particles (median 1.5 µm) were obtained using 60% amplitude ultrasound. For all conditions, except Ms120, the particles obtained had similar sizes and a narrow size distribution. The varied size of the particles that correlate with the increase in shear rate was an expected phenomenon. This correlation is consistent with the findings of the literature [10].

All produced particles tended to agglomerate, and this was especially visible for the smaller So60 particles (FIG. 1D). The shape of the particles was diverse. Some of the particles had irregular shapes, some had cuboid shapes, and some were rounded. Calcium carbonate particles which have a form of thermodynamically unstable vaterite undergo phase transition into stable calcite [9,10]. It is specifically visible in our SEM images: So20 and So60 particles were subjected to air drying and during that time their phase transition occurred (FIG. 1C, D). Only a small portion of the So20 particles remained rounded (i.e., vaterite), and in the case of So60, all the particles had a cuboid shape (i.e., calcite).

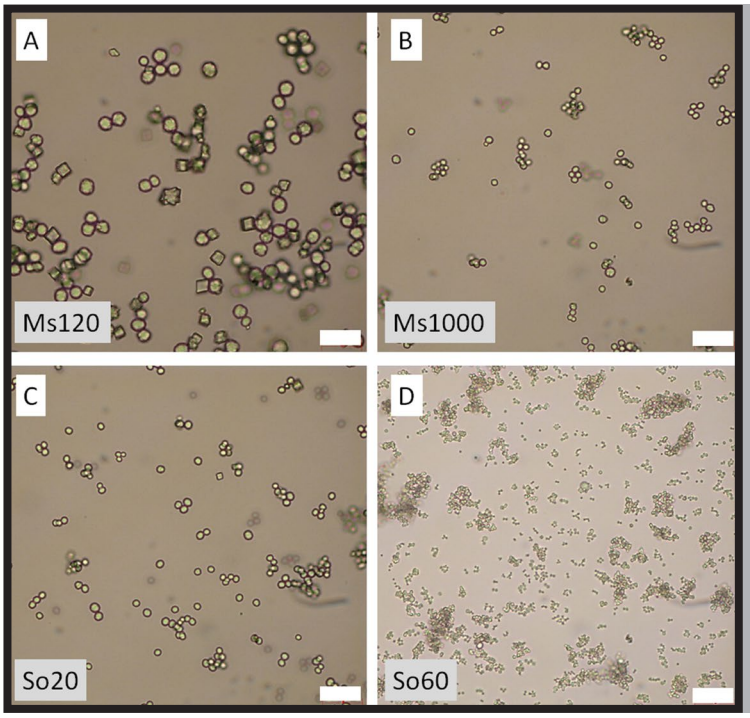

FIG. 1. Optical microscopy images of the unloaded calcium carbonate particles produced at different conditions: slow magnetic stirring (120 rpm, Ms120) (A); fast magnetic stirring (1000 rpm, Ms1000) (B); 20% amplitude sonication (So20) (C); 60% amplitude sonication (So60) (D). Scale bar = 20 μm.

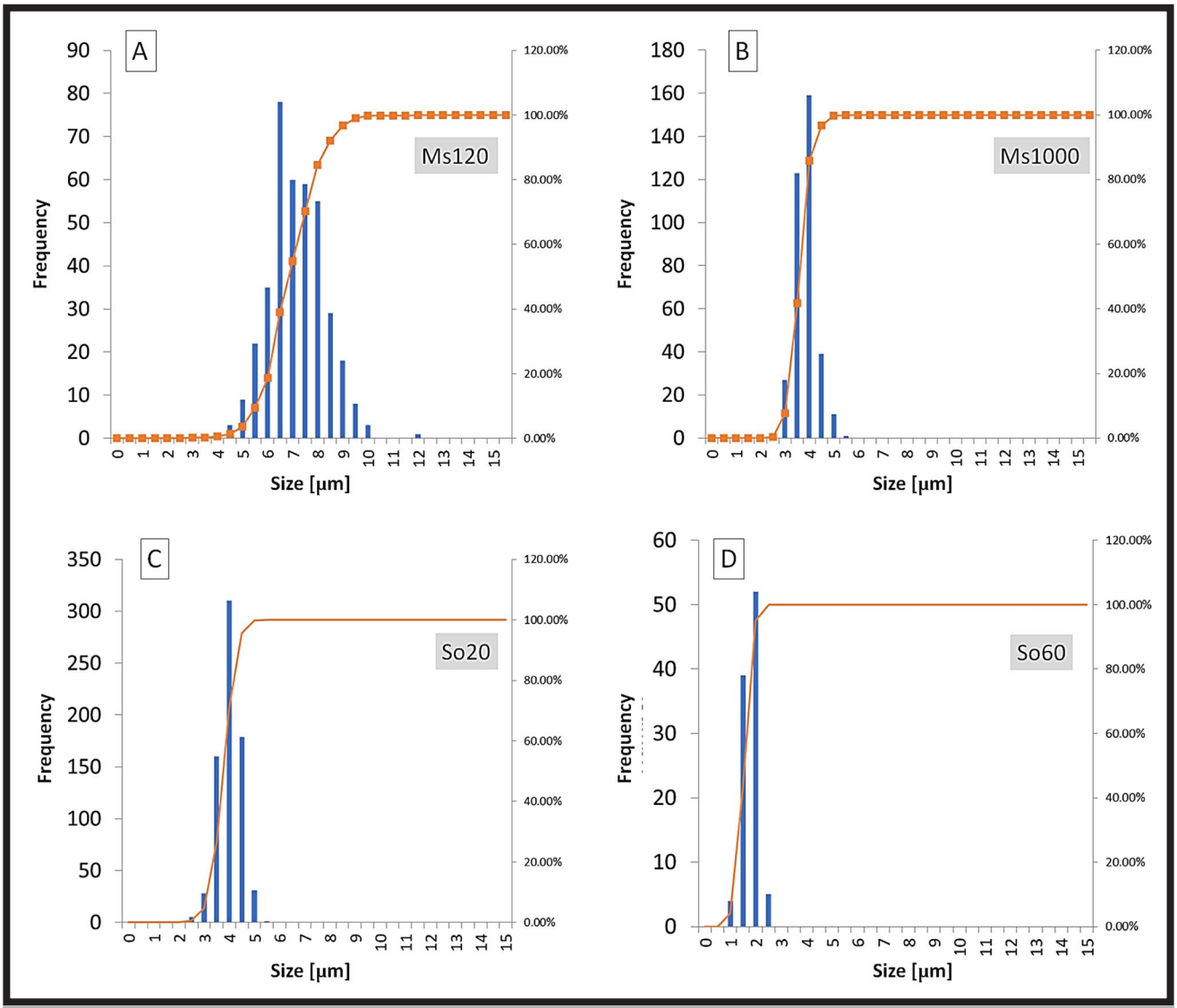

FIG. 2. Histograms of the empty calcium carbonate particles. Slow magnetic stirring particles (120 rpm, Ms120) (A); fast magnetic stirring particles (1000 rpm, Ms1000) (B); 20% amplitude sonicated particles (So20) (C); 60% amplitude sonicated particles (So60) (D).

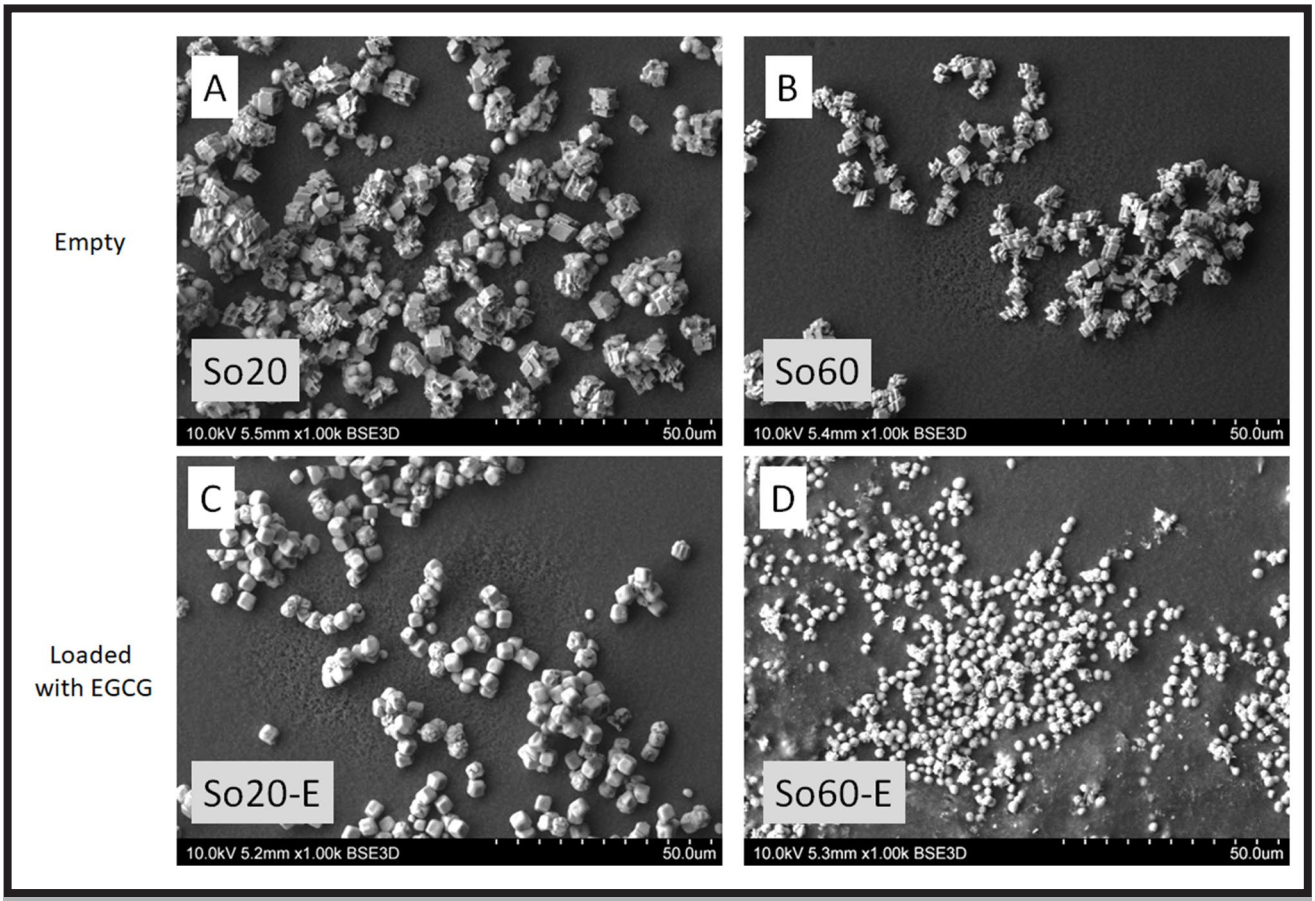

FIG. 3. SEM images of calcium carbonate particles: empty 20% amplitude sonicated (So20) (A), empty 60% amplitude sonicated (So60) (B), EGCG-loaded 20% amplitude sonicated (So20-E) (C), and EGCG-loaded 60% amplitude sonicated particles (So60-E) (D). Scale bar = 50 µm.

In the presence of EGCG phase transition was inhibited for So20, as well as for much smaller So60 (FIG. 3). Most of the particles remained rounded and only a small portion of the particles had a cuboid shape. This effect can be explained by the fact that the organic compound EGCG is adsorbing on a Ca_2CO_3 surface, therefore stabilizing the structure, size, and shape and preventing its phase transition into calcite.

As shown by the Folin-Ciocalteu method, the EGCG content in So20 and So60 was 1.1% and 1.3%, respectively. EGCG release studies showed that between 60% and 70% of this component was released during the first 24 h of incubation, however, a significant amount was still released after 14 days (FIG. 4). For So20 almost 95% EGCG was released during the experiment time, but for So60 the level of 75% was only reached. The reason might be the lower accessibility of smaller particles to external incubation fluid, due to their higher tendency for agglomeration resulting from the higher surface area and thus higher surface free energy. The mechanism of EGCG encapsulation and release from these particles is not clear. We can speculate that EGCG can be physically entrapped inside precipitated particles or adsorbed on the surface of small calcium carbonate crystallites because of their large surface area and thus high surface free energy. The release mechanism can be related to phase changes in calcium carbonate from hexagonal vaterite to rhombohedral calcite (smaller to bigger crystals) and EGCG desorption.

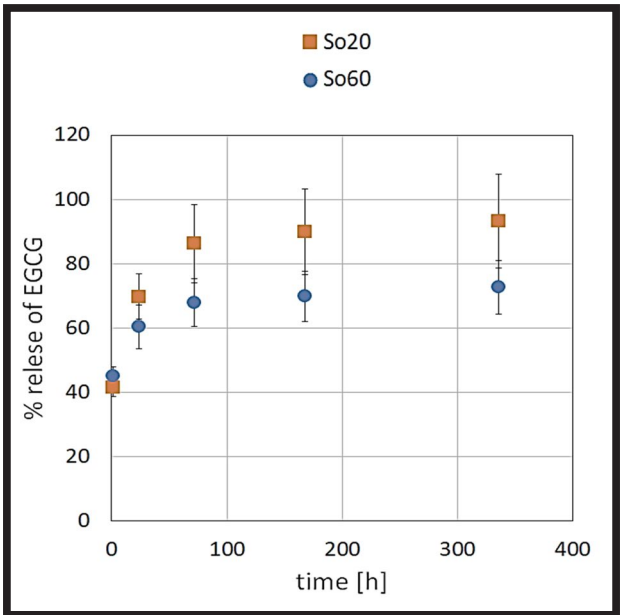

FIG. 4. Release of EGCG from calcium carbonate particles: EGCG-loaded 20% amplitude sonicated (So20-E) and EGCG-loaded 60% amplitude sonicated particles (So60-E) during 14 days of incubation in PBS at 37°C.

The particles obtained by the 60% amplitude sonication method, both unloaded and loaded with EGCG (So60 and So60-E, respectively) were tested in contact with osteoblast-like cells in 3 different concentrations of EGCG: 1, 0.5, and 0.25 mg/ml. The same amount of particles not loaded with EGCG was also used for comparison. As a control, cells cultured in pure medium were evaluated. The Alamar Blue viability test (FIG. 5A) showed a significant decrease in cell viability for all cases as compared to the control. The loss of viability was much higher for empty So60 and reached around 60%. Concomitantly, these samples exhibited the highest cytotoxicity as studied by the LDH assay (FIG. 5B). Interestingly, EGCG-loaded particles (So60-E) produced under the same conditions as So60 were characterized by significantly higher cell viability and lower cytotoxicity. For both unloaded So20 and EGCG-loaded particles (So20-E), cell viability was not significantly different. Intriguingly, cell viability did not depend on the amount of particles added to the cell culture wells. On the other hand, the tendency was visible with particle content in the LDH cytotoxicity test (FIG. 5B) for all samples. However, cytotoxicity was only elevated for So60 unloaded samples compared to the control. Other samples had a similar or lower LDH level than the control.

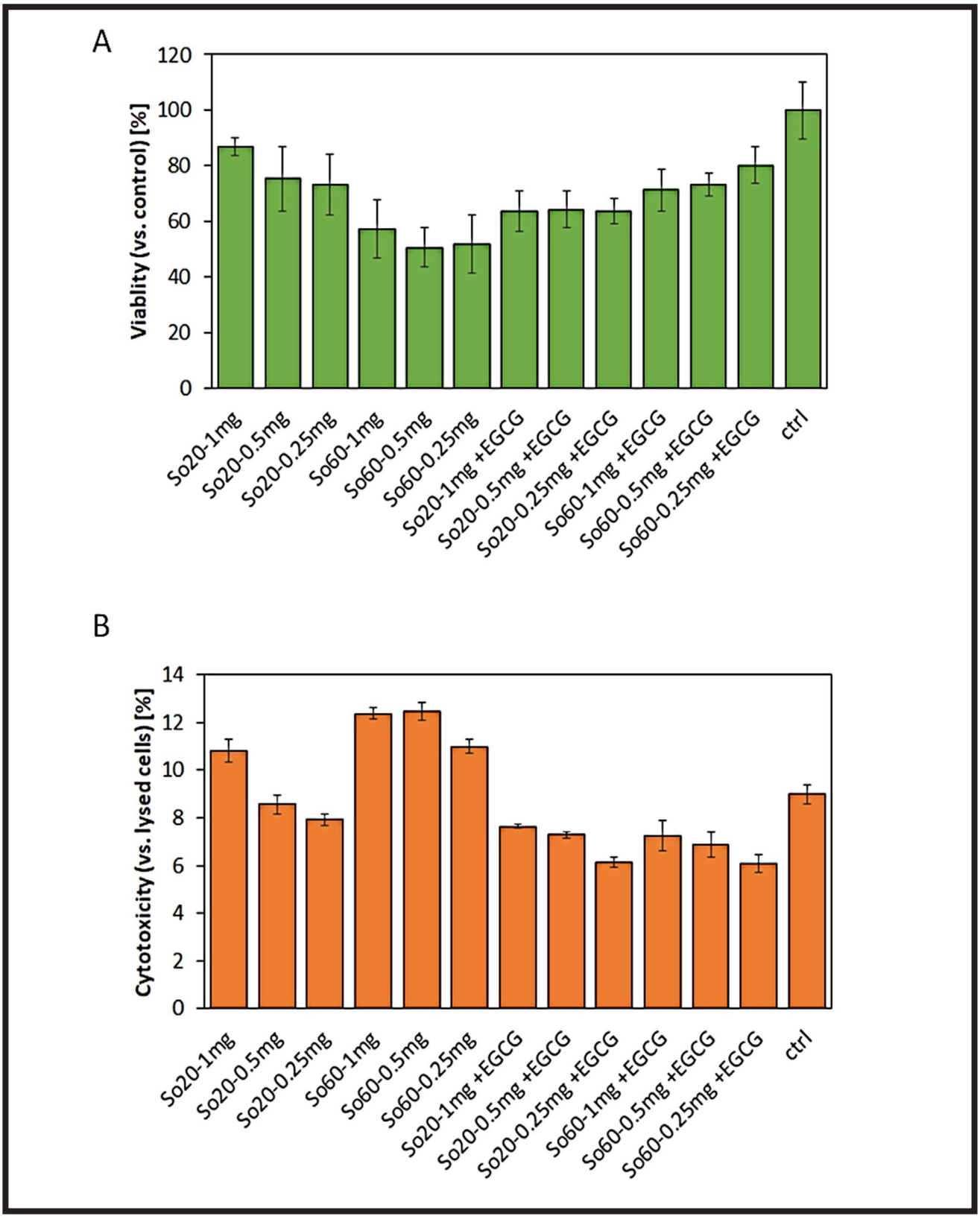

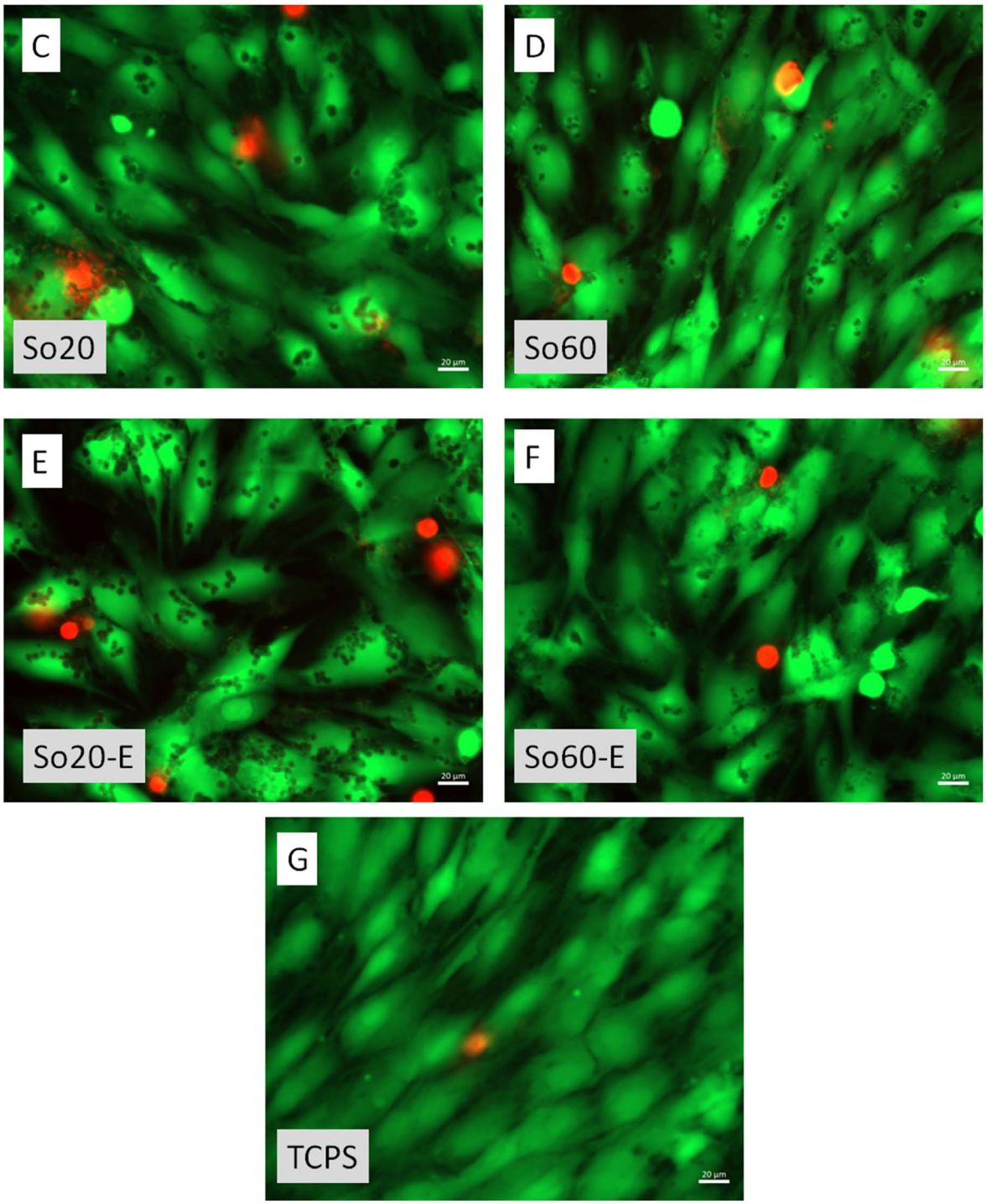

FIG. 5. In vitro results of MG-63 cells after 2 days of culture in contact with So20 and So60 unloaded and EGCG-loaded microparticles at 3 different concentrations: 1, 0.5 and 0.25 mg/ml in contact. Viability test (A) and LDH cytotoxicity test (B). All samples were significantly different as compared to control conditions according to ANOVA, $p < 0.05$. Live/dead staining for 1 mg/ml particles concentration (C-G) in comparison with culture in control conditions (tissue culture polystyrene, TCPS): green – live cells, red – dead cells. Scale bar = 20 µm.

The live/dead staining test showed that there was only a modest change in morphology between the culture with particles compared to the control (FIG. 5C-G). The spreading area of the cells appeared slightly smaller and there were more free spaces between the cells. The results showed that the particles were found non-cytotoxic. The decrease in viability was probably related to accessibility to the surface that was hindered by the particles present. A significant cytotoxic effect was observed for the unloaded So60 samples. This effect can be attributed to the rough and edgy surface of highly crystalline calcite particles that predominate in this case. The EGCG content in the particles did not negatively affect viability nor provoked an elevated cytotoxic effect of the particles on studied cells. On the contrary, protection of their initial spherical shape had a positive effect on proliferation and significant lowering of LDH level even compared to the control. This beneficial effect can also be derived from EGCG biological activity as it has a strong antioxidant effect [11,12].

Hydrogels modified with mineralization and particles

Particles obtained by ultrasound loaded with EGCG were further tested as the GG-Gel hydrogel modifier. 0.15% w/v of the particles was added before gelation occurred. The gelation of the hydrogel was relatively fast (less than 2 min), which reduced the effect of possible sedimentation. The cylindrical samples were further mineralized enzymatically to introduce calcium phosphate deposits inside and create composite material for bone regeneration.

After freeze-drying porous hydrogel scaffolds were obtained (FIG. 6). The particles were distributed in the hydrogel relatively homogeneously, which was especially visible for the smaller So60 particles (FIG. 6C, E). For the samples without particles added, the pore walls were smooth (FIG. 6A).

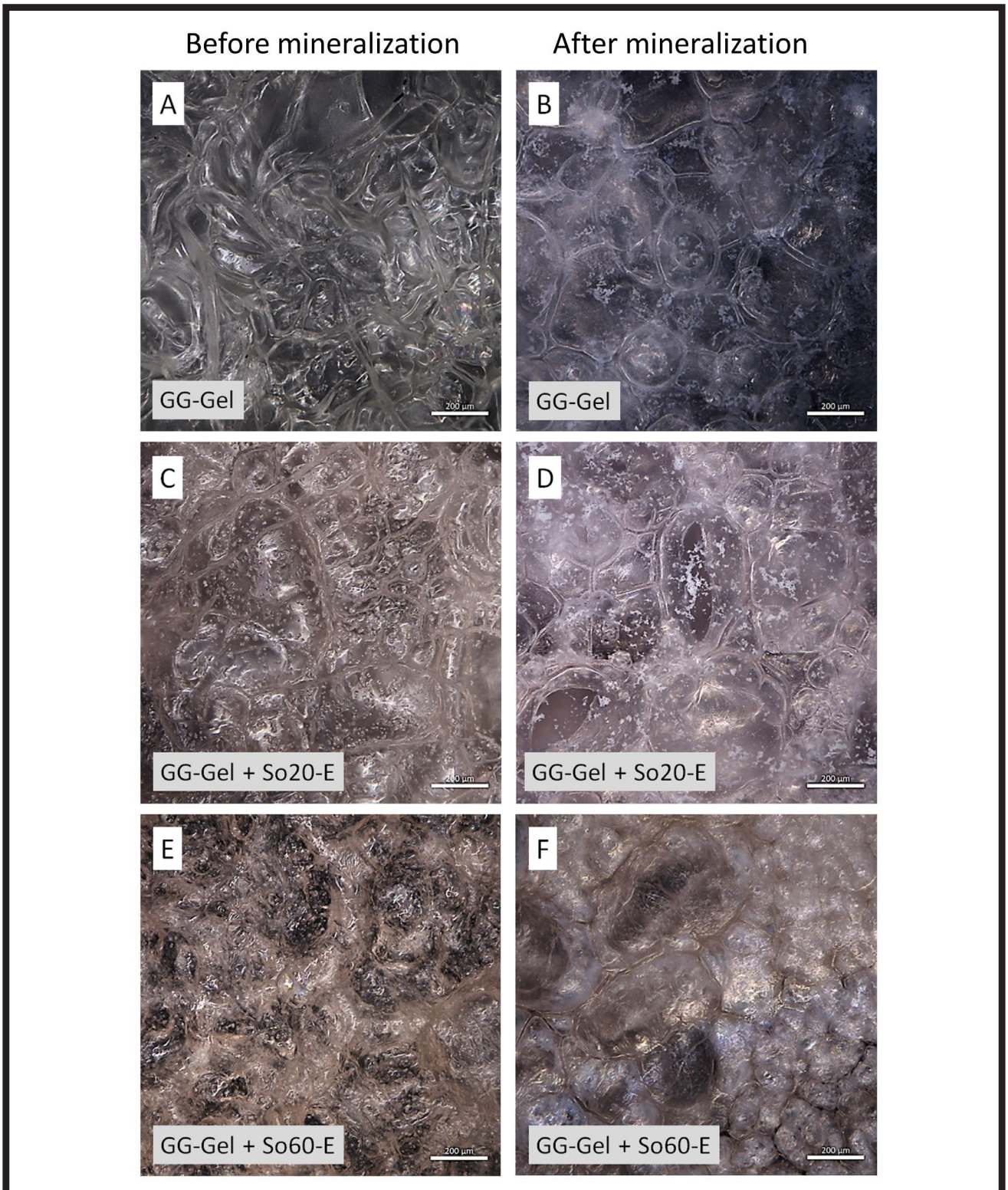

FIG. 6. Morphology by SEM of GG-Gel hydrogels: without particles before (A) and after mineralization (B) and freeze-drying. Morphology of hydrogels with particles loaded with EGCG So20-E and So60-E, before (C, E) and after mineralization (D, F) and freeze-drying. Scale bar = 200 µm.

The SEM images (FIG. 7) on cryosection revealed that the pores were 200-500 μm in size for the unmodified hydrogel (FIG. 7A) and the one modified with So20-E (FIG. 7C), while much smaller, i.e. 50-100 μm, for the So60-modified hydrogel (FIG. 7E). The presence of So60-E particles also led to a denser and collapsed structure. The particles were not clearly visible on the SEM images as they might have been closely entrapped within the hydrogel matrix.

Mineralization introduced precipitates of inorganic phosphates for all materials, as shown in our previous studies [5,8,13]. Bigger precipitates were visible in GG-Gel and GG-Gel+So20 samples (FIG. 6B, D). No precipitates outside the hydrogel were visible for GG-Gel+So60 (FIG. 6F). However, in this case mineralization also took place, judging by SEM images and the change in colour of the scaffolds. SEM images (FIGs. 7B, D, F) showed that in all cases mineralization led to the thickening of scaffold walls and caused calcium phosphate deposition on a surface. For GG-Gel+So60, precipitates were again hardly visible.

The presence of particles clearly affected the freeze-drying and mineralization process. Small particles can act as nucleation sites for calcium phosphate crystallization during mineralization. It can be observed for smaller So60 particles as their size is around 1-2 μm. In that case, the mineralization is more homogeneous, and there are no precipitates inside the pores. Pore sizes in the nonmineralized material were much smaller but after mineralization this effect was reversed. All mineralized samples had a similar pore size. The reason for this effect remains unclear. Bigger particles did not affect the mineralization process, and obtained porosity was comparable with that of the non-modified GG-Gel hydrogel. It may be related to a smaller overall exposed surface area and a lower tendency to recrystallize in aqueous conditions. GG-Gel+So60 samples after mineralization had a smoother surface compared to other materials.

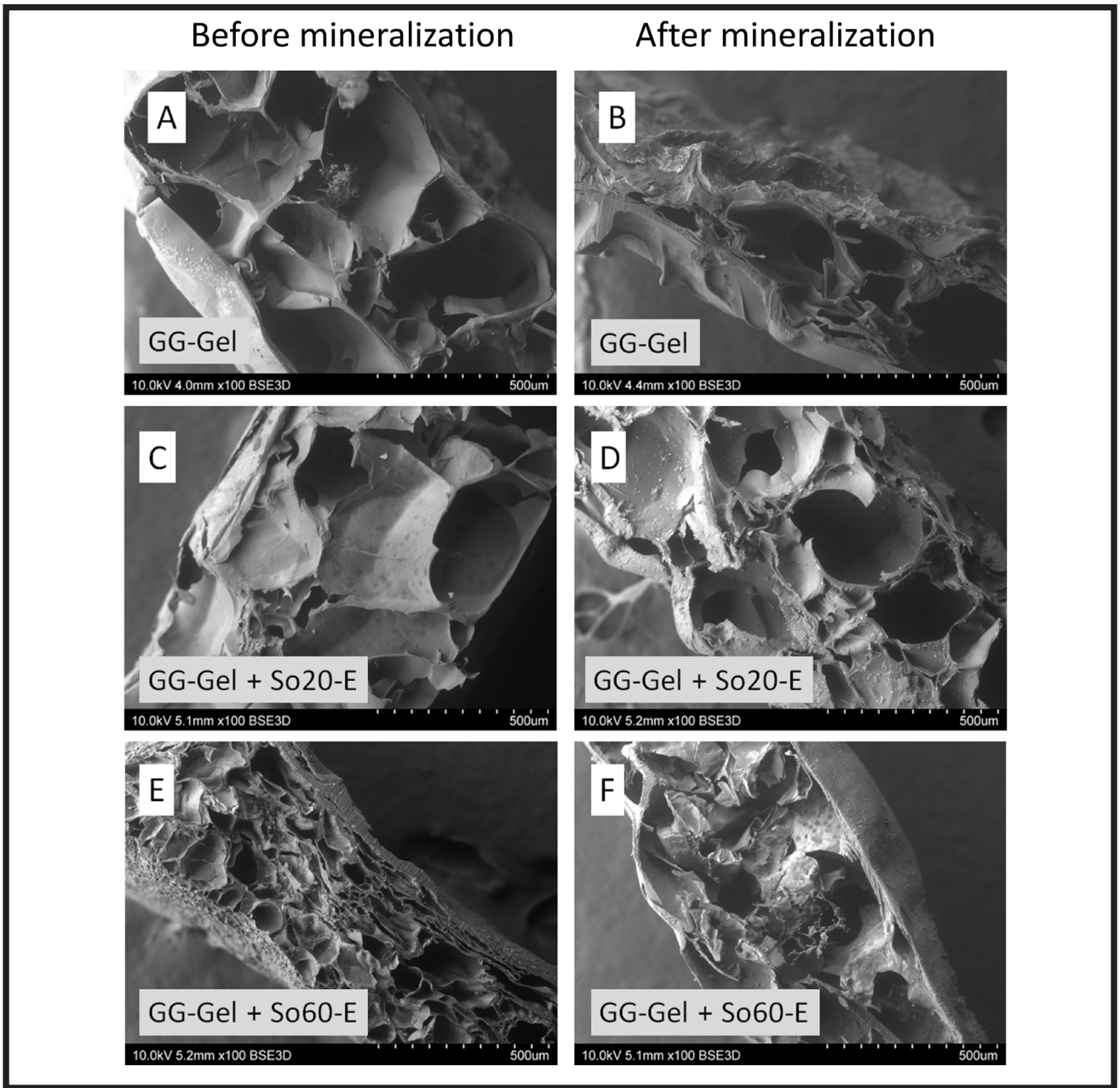

FIG. 7. SEM images of cross-sectioned freeze-dried GG-Gel hydrogels without particles before (A) and after mineralization (B). Morphology of hydrogels with particles So20-E and So60-E, before (C, E) and after mineralization (D, F). Scale bar = 500 μm.

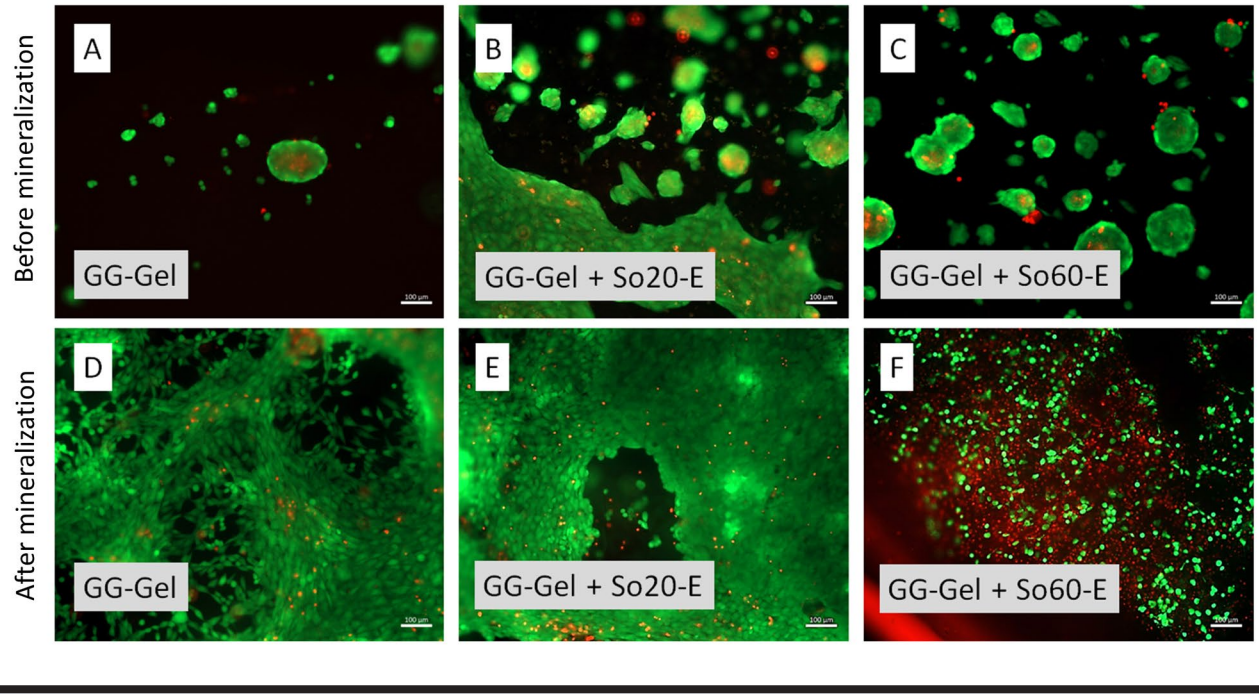

FIG. 8. Live-dead staining of 7-day culture of MG-63 on the surface of GG-Gel materials without particles (A, D) and with particles S020-E (B, E) and So60-E (C, F), prior (A, B, C) and after mineralization (D, E, F). Scale bar = 200 μm.

Live/dead staining of MG-63 culture in materials revealed significant differences (FIG. 8). The introduction of particles into the material led to an increase in cell adhesion compared to the unmodified GG-Gel (FIG. 8A, B, C). Additional mineralization improved cell adhesion, except for the GG-Gel+So60-E sample (FIG. 8D, E, F). However, this deteriorating effect did not prevent cell agglomeration as in the case of nonmineralized sample. The presence of a small number and separated cells with a high percentage of dead cells may indicate a different reason for such a phenomenon. In fact, the surface of the hydrogel could be more mineralized than the rest of the hydrogel because mineralization proceeding in the presence of nucleation sites is more efficient. The higher level of mineralization may negatively affect the gel stability in an aqueous solution. Stronger mineralization can be toxic. In addition, swelling of interior parts of the scaffold can cause cracking of a rigid calcium phosphate layer on the surface and disintegration of the sample structure. Cells within deeper cracks could not have access to nutrients or lack stable support, which is crucial for anchorage-dependent cells, such as osteoblasts. This hypothesis is supported by the fact that a lot of dead cells were visible below the hydrogel surface.

Conclusion

In our study, calcium carbonate microparticles of various sizes were produced by alternating shear force during the precipitation process. The feasibility of introducing EGCG into microparticles was confirmed, as well as its gradual release. EGCG had a beneficial effect on the stability of calcium carbonate microparticles, preventing its phase transformation from vaterite into calcite. The biocompatibility of smaller particles was confirmed in cell culture. The introduction of EGCG had a beneficial effect in reducing the cytotoxicity of the crystalized particles. Particles introduced into the hydrogel influenced the microstructure of the scaffolds, lowering the pore size. The mineralization process was also affected by the presence of the microparticles that can act as nucleation sites for calcium phosphate crystal formation, causing the mineralization to be more homogenous. The particles present in the hydrogel significantly improved cell adhesion. Mineralization with calcium phosphate combined with calcium carbonate microparticles addition had even more substantial effect on scaffolds microstructure and biological properties.

Our study confirmed that the GG-Gel hydrogel can be enriched with EGCG-loaded $CaCO_3$ microparticles and this material can be further modified with enzymatic mineralization introducing calcium phosphates. These modifications can have a positive effect on biocompatibility with bone cells, thus promising to obtain scaffolds for bone tissue regeneration.

Acknowledgements

This study was supported by the National Science Centre Poland (No 2018/29/N/ST8/01544) and by the program "Excellence Initiative–Research University" for AGH University of Science and Technology, Kraków, Poland.

ORCID iD

K. Pietryga: https://orcid.org/0000-0002-6343-8849
A.-A. Panaite: https://orcid.org/0009-0007-4073-370X
E. Pamuła: https://orcid.org/0000-0002-0464-6189

References

[1] Florencio-Silva R., Sasso G.R. da S., Sasso-Cerri E., Simões M.J., Cerri P.S.: Biology of Bone Tissue: Structure, Function, and Factors That Influence Bone Cells. BioMed Res Int 2015 (2015) 1–17. https://doi.org/10.1155/2015/421746.
[2] Roseti L., Parisi V., Petretta M., Cavallo C., Desando G., Bartolotti I., et al.: Scaffolds for Bone Tissue Engineering: State of the art and new perspectives. Mater Sci Eng C 78 (2017) 1246–1262. https://doi.org/10.1016/j.msec.2017.05.017.
[3] Jiang S., Wang M., He J.: A review of biomimetic scaffolds for bone regeneration: Toward a cell-free strategy. Bioeng Transl Med 6 (2021) https://doi.org/10.1002/btm2.10206.
[4] Douglas T.E.L., Messersmith P.B., Chasan S., Mikos A.G., de Mulder E.L.W., Dickson G., et al.: Enzymatic Mineralization of Hydrogels for Bone Tissue Engineering by Incorporation of Alkaline Phosphatase. Macromol Biosci 12 (2012) 1077–1089. https://doi.org/10.1002/mabi.201100501.
[5] Pietryga K., Reczyńska-Kolman K., Reseland J.E., Haugen H., Larreta-Garde V., Pamuła E.: Biphasic monolithic osteochondral scaffolds obtained by diffusion-limited enzymatic mineralization of gellan gum hydrogel. Biocybern Biomed Eng 43 (2023) 189–205. https://doi.org/10.1016/j.bbe.2022.12.009.
[6] Dorati R., DeTrizio A., Modena T., Conti B., Benazzo F., Gastaldi G., et al.: Biodegradable Scaffolds for Bone Regeneration Combined with Drug-Delivery Systems in Osteomyelitis Therapy. Pharmaceuticals 10:96 (2017) https://doi.org/10.3390/ph10040096.
[7] Villarreal-Otalvaro C., Coburn J.M.: Fabrication Methods and Form Factors of Gellan Gum-Based Materials for Drug Delivery and Anti-Cancer Applications. ACS Biomater Sci Eng 2021:acsbiomaterials.1c00685. https://doi.org/10.1021/acsbiomaterials.1c00685.
[8] Douglas T.E.L., Pilarz M., Lopez-Heredia M., Brackman G., Schaubroeck D., Balcaen L., et al.: Composites of gellan gum hydrogel enzymatically mineralized with calcium-zinc phosphate for bone regeneration with antibacterial activity: Antibacterial hydrogels mineralized with Ca-Zn phosphate. J Tissue Eng Regen Med 11 (2017) 1610–1618. https://doi.org/10.1002/term.2062.
[9] Fadia P., Tyagi S., Bhagat S., Nair A., Panchal P., Dave H., et al.: Calcium carbonate nano- and microparticles: synthesis methods and biological applications. 3 Biotech 11:457 (2021) https://doi.org/10.1007/s13205-021-02995-2.
[10] Sovova S., Abalymov A., Pekar M., Skirtach A.G., Parakhonskiy B.: Calcium carbonate particles: synthesis, temperature and time influence on the size, shape, phase, and their impact on cell hydroxyapatite formation. J Mater Chem B 9 (2021) 8308–8320. https://doi.org/10.1039/D1TB01072G.
[11] Honda Y., Takeda Y., Li P., Huang A., Sasayama S., Hara E., et al.: Epigallocatechin Gallate-Modified Gelatin Sponges Treated by Vacuum Heating as a Novel Scaffold for Bone Tissue Engineering. Molecules 23:876 (2018) https://doi.org/10.3390/molecules23040876.
[12] Song L., Xie X., Lv C., Khan A. ur R., Sun Y., Li R., et al.: Electrospun biodegradable nanofibers loaded with epigallocatechin gallate for guided bone regeneration. Compos Part B Eng 238 (2022) 109920. https://doi.org/10.1016/j.compositesb.2022.109920.
[13] Pietryga K., Costa J., Pereira P., Douglas T.E.L.: Promotion of bone cells growth on gellan gum hydrogels by enzymatic mineralization. Eng Biomat 125 (2014) 6–12.